*Sensors & Transducers, Vol. 274, Issue 3, October 2026, pp. 61-75*

www.sensorsportal.com

**Sensors & Transducers**

Published by IFSA Publishing, S. L., 2026
http://www.sensorsportal.com

# Performance Analysis of Hybrid Beamforming Optimization Algorithms for mm-Wave Massive-MIMO Systems

**[1] Girija SHANKAR SAHOO, [1] Anumoy GHOSH and [2,*] Abhishek SAHA**

[1] Department of Electronics Communication and Engineering,
National Institute of Technology, Mizoram, India
[2] Department of Electronics and Communication Engineering,
Dream Institute of Technology, Kolkata, India
E-mail: abhishek.saha@dreaminstituteonline.edu.in

*/Received: 9 May 2026 /Revised:21 June 2026 /Accepted: 19 Oct. 2026 /Published: 30 Oct. 2026*

**Abstract:** The hybrid beamforming(HBF) in millimeter wave (mmWave) MIMO wireless communication system is an emerging technique used in modern communications system to fulfill the demandas of high data rate and low latency. This article investigates the best suited optimization technique to improve the beamforming gains thereby reducing the propagation loss. The investigation was conducted on the analysis and implementation of General Eigen Value Decomposition (GEVD), Orthogonal Matching Pursuit (OMP), and Manifold Optimization HBF techniques at precoder and combiner. Scattered channel model is used in this work. 2×2, 4×4, 8×8 and 16×16 massive MIMO antenna array structures are considered at the transmitter. Data streams ranging from 1 to 4 are considered. The performance is evaluated on the basis of spectral efficiency, mean square error (MSE) and Bit Error Rate (BER). Effects of massive MIMO array size and data streams on the performance metrics of the HBF algorithms are demonstrated with analysis. The performance of the HBF algorithms is compared with full digital beamforming technique to comprehend their relative advantages over the sophisticated and power hungry digital beamforming technique.

**Keywords:** Hybrid beamforming, Multi input multi output system, Manifold optimization, Orthogonal matching pursuit, Geeneralized eigenvalue decomposition.

## 1. Introduction

The next-generation mmWave wireless communication system is provide a promosing solution for modern communication systems that require extremely high data rates and bandwidth to accommodate large number of user and provide fast communication channels. These goals can be met if the communication spectrum is shifted to the mm-wave region using massive multi-input and multi output (MIMO) systems. The mm-wave massive MIMO system also increases the spectral efficiency and decreases latency by manifold [1]. Numerous numbers of antenna element use in massive MIMO system, generates significant interference that adversely affects the channel capacity and the performance of 5G communication systems [1]. Beamforming technique is employed to circumvent this problem which reduces the multipath fading and inter channel interference by concentrate the signal in desired direction [2]. This Beamforming realized by assembling the elements in the massive MIMO configuration in an organized array. Beam in a specific direction are added and subtracted in the other direction. Beamforming algorithm implemented at baseband and RF modules of the MIMO systems can also reduce path loss. Thus, beamforming is an effective technique which when used in conjunction

with massive MIMO system provides very high spectral efficiency and reduces the bit error rate [3].

## 1.1. MIMO

In the new in future of communication increasing demand of wireless communication services, there is an increased requirement of high data rate and energy efficiency. The massive MIMO wireless communication technology fulfills this requirement. Fig. 1, shows the massive MIMO cellular system with a station (BS) and multiple user equipment (UE) devices equipped with antenna array. Multiple UEs are scattered throughout the cell area. Each UE is equipped with multiple antennas, allowing it to receive signals with spatial diversity. Wireless communication link between BS and UEs with beamforming techniques are used to focus the transmitted signals towards the intended UE, optimizing signal strength and minimizing interference [4]. Successfully implement the mmWave massive MIMO technology support broad range of technology services including machine to machine (M2M), Internet on vehicles (IoV), device to devices (D2D) and backhaul access cellular network. Efficient beamforming techniques are to be employed to provide the capability of higher spectral and energy efficiencies.

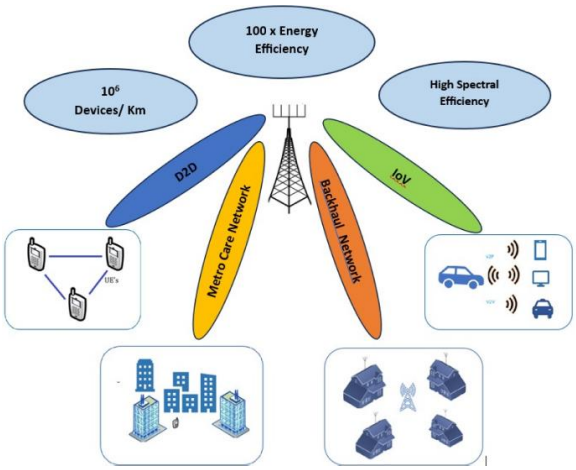



**Fig. 1.** An example of massive MIMO cellular communication system.

## 1.2. Hybrid Beamforming

Hybrid beamforming was achieved using initial stage the baseband precoder and second stage is RF precoder are used for pre signal processing and phase controls, respectively. The hybrid approach tradeoffs the advantages of both the configuration analog and digital beamformer. Based on the grouping of the antennas, there is cluster-based fully connected and partially connected antenna hybrid beamforming technique. In the cluster-based hybrid technique balance the hardware complexity and performance by reducing the number of RF chain [2, 5]. Fully connected hybrid beamforming increases the number of the RF chain, while it provides the highest level of the flexibility and adaptability [6]. In partially connected hybrid beamforming antennas are divided in small groups. Each group is connected to a shared RF chain and group have different RF beamforming weight to support spatial multiplexing. Partially connected beamforming provide the balance between performance and hardware complexity [5, 7].

Initially, analog beamforming was the preferred technique, but it gradually shifted to digital beamforming [8, 9]. In massive MIMO scenario, disadvantage of analog and digital beamforming with respect to hardware complexity and power requirement respectively [10] becomes significant. Thus, the hybrid beamforming (HBF) technique, where digital baseband precoder and analog RF precoder [10] avoiding the disadvantages of both. HBF as compared to full digital beamforming is difficult in term of optimizing four variables at baseband and RF module [11, 12]. Existing problems on HBF algorithms solve by breaking actual problem into subproblem for precoding and combining section in the transmitter and receiver sections [13]. One popularly used approach to hybrid beamforming design is singular value decomposition and Euclidean distance of hybrid beamformer with optimal beamforming [14]. Orthogonal matching pursuit (OMP) is used for spatially sparse precoding and combining algorithm to solve by matrix factorization problem [14]. In [15], a low complexity manifold optimization algorithm discussed, other than the matrix factorization approach. Iterative algorithm is designed for closed form solution of beamformer with original objective function [14, 16].

All the previous works in the development of HBF algorithms are based on maximizing the spectral efficiency. Other important performance metrics beside the spectral efficiency are Mean Square Error (MSE) and Bit Error Rate (BER) that can be controlled by the optimization of precoding and combining weights at precoder and RF sections respectively [17-19]. In practical systems, some modulation scheme is used for data transmission and thus MSE is an important metric to measure the transmission reliability [20]. Signal to interference noise ratio (SINR) and BER metrics are related to MSE in the beamforming design for multiple data. Thus the MSE and BER metrics as alternate objectives of spectral efficiency [18-20] for HBF algorithms to compare their performance with respect to full digital beamforming. Precoding matrices optimized by minimizing the MSE can also improve the spectral efficiency [21]. The traditional low complex Othogonal Matching Pursuit (OMP) dictionary based beamselction method to approximate the digital precoder. The four variables on the beamformer are optimized instead of factorizing the optimal full digital beamforming. HBF is optimized the MMSE enhance the performance [22]. In the HBF design approach, the minimization problem of MSE is decomposed into

subproblem hybrid precoding and combining. The selection of hybrid beamforming algorithm based on reduced complexity and better performance. Manifold Optimization (MO) Hybrid Beamforming approach to minimized the Euclidean distance between the optimal and hybrid beamformer to achieve the convergence [23]. The purpose of the Hybrid beamforming algorithm (HBF) is optimizing the MSE without any constraint of the space feasible solution and achieve the higher performance. We seek low complexity algorithm Generalized Eigen Value Decomposition (GEVD) beamforming matrix optimize column wise column to avoid the complexity and achieve the high data rate. Key issues and problem statement identified in previous work as follows:

- In traditional beamforming technique, large scale antenna array system encounters the high computational complexity and suboptimal performance. Hybrid beamforming, which combine digital and analog beamforming to strike balance between performance and complexity;
- Hybrid Beamforming algorithm optimize the beamforming process by incorporate the MMSE criteria to mitigate the interference and noise. While maximizing signal quality, thus improving overall system performance and robustness to the channel variation;
- Practical implementation of hybrid beamforming, complexity analysis is crucial parameter to tradeoff between sustainability of system and performance.

In this article several hybrid beamforming technique discussed for mmWave massive MIMO system. The Orthoganal Matching Pursuit (OMP) hybrid beamforming leverage the channel sparsity, where only few dominant path exist to approximate the optimal digital precoder by using dictionary based selection. The OMP hybrid beamforming has lower computational efficiency and its performance degarde with increasing data stream and channel correlation. The itrative based Manifold Optimization (MO) and Generalized Eigen Value Decomposition (GEVD) hybrid beamforming better performamnce over traditional beamforming technique. The GEVD Hybrid beamforming method gives the attractive trade-off between and complexity.

The most of the studies focus on either maximization of spectral efficiency or MMSE optimization under fixed antenna configuration and simulation assumption. Which makes difficult for direct comparison and to choose better hybrid beamformer configuration. Therefore, our work present unified framework to measure the performance of OMP, MO and GEVD hybrid beam forming algorithm under identical channel condition, RF chain constraint and power allocation. The contribution of our work summarized as follows:

- Design and analysis of 2×2, 4×4, 8×8 and 16×16 rectangular massive MIMO antenna array operating 28 GHz frequency;
- Implementation of Hybrid beamforming algorithm OMP, MO and GEVD under common MMSE base framework;
- Investigate the performance metric spectral efficiency, MSE, BER and Energy efficiency computational complexity varying antenna array size and data stream;
- Compare the performance and trade-off between performance and computation cost among the hybrid beamforming algorithm. The work identify selection of practical beamformer for future mmWave massive MIMO system.

This work extends our previous study in the persented in the IEEE Wireless Antenna and Microwave Propogation (WAMS 2022) [21], where antenna array design for hybrid beamforming investigated. In the persent work, we significantly extends that study by implementation of hybrid beamforming algorithms and evaluating the performance of these algorithm in term of spectral efficiency (SE), mean square error (MSE), bit error rate (BER) and energy efficiency (EE). This article is structure as follows: Section 2 elucidates the channel modeling and massive MIMO antenna array considered for the proposed work. Section 3 gives the detailed analysis of the three HBF algorithms and deriving the SINR, SE, MSE and BER thereof. Section 4 illustrates the simulation results relying on the analysis in Section 3 and presents a performance evaluation and comparison among the HBF algorithms based on SE, MSE and BER. Section 5 concludes this work with final comments. Throughout this article, uppercase letter and lowercase letters are represent the matrices, column vector and scalar value. The subscripts $()^T$,$()^*$ and $()^H$ represent transpose matrix, complex conjugate and hermitian matrix. tr() and ||.|| denote the trace of the matrix and Euclidean norm of the vector respectively. Conjugate gradient function is $\nabla()$ and E{} indicates expectation operator. $[A]_{i,j}$ denotes the $i-j^{th}$ entry of a matrix A.

## 2. Designing and Modelling of Massive MIMO System

The massive MIMO mmWave communication technology increases the spectral efficiency and channel capacity significantly by increase the antenna element. This technique encountered with certain challenges such as interference caused by deployment of large antenna array. Beamforming technique popularly used to mitigate the interference challenge in massive MIMO system [12, 14]. This articler discussed, the shape and size of antenna array play pivotal role in characteristics channel model. In MIMO system, spacing between antenna element in rectangular antenna array determine the mutual coupling and channel matrix. For scenario user equipment positioned very closely, correlation between user equipment higher as compared to independent identical distributed (i.i.d) Rayleigh

channel. This can be minimized and uncorrelated by large antenna array.

## 2.1. Channel Model

The correlation-based channel model used to analyze performance and the statistical properties of wireless communication. it is also used for the design theoretical model when UE employs single antenna further extended to UE with multiple antenna. A list of symbols is presented in Table 1.

**Table 1.** List of Symbols.

| Symbol | Definition |
|---|---|
| $G$ | Channel Matrix |
| $D$ | Propagation Matrix |
| $\beta_k$ | Large scale fading factor |
| $\phi$ | Gain constant |
| $d_k$ | Distance between the $k_{th}$ UE and the base station |
| $\xi_k$ | Shadow fading component |
| $H$ | Fast fading channel matrix |
| $h_k$ | Channel vector for $\boldsymbol{k^{th}}$ UE |
| $\alpha$ | Path loss exponent |
| $R_k$ | Steering Vector at different angle AoA |
| $\theta_{k,i}, \phi_{k,i}$ | Elevation and Azimuthal AoA |
| $\lambda$ | Carrier wavelength |
| $d$ | Distance between adjacent antennas |

A uplink channel uses $K$ number UEs with single antenna and base station equipped with $N$ antennas, where NLoS channel formulize as [24]

$$G = H \times D^{1/2}, \quad (1)$$

where $D$ is the propagation matrix given as [24].

$$D = diag\{\beta_1, \beta_2, \dots, \beta_k\}, \quad (2)$$

where $\beta_k = \phi d_k^{-\alpha} \xi_k$, $\Phi$ is gain constant, $d_k$ is the distance between $k^{th}$ UE to base station, $\alpha$ is the path loss, and $\xi_k$ is fading loss component with $10\log 10\xi_k \sim N(0, \sigma_{sh}^2)$ and $H \in \zeta^{N \times K}$ is fading channel matrix.

The elements of the channel matrix $H = [h_1, h_2 \dots, h_k]$. Here, antenna correlation is determined by clustering and scattering environments [25]. Where the channel vector $h_k$ for the $k^{th}$ UE is correlation matrix multiplied by standard complex Gaussian vector as

$$h_k = R_k v_k;\ k = 1,2, \dots k \quad (3)$$

Steering matrix is $R_k = \zeta^{N \times D_k}$, where $D_k$ steering vectors and complex gaussian vector is $v_k \sim \xi N(0, I_{D_k})$. Steering matrix $R_k$ for $k^{th}$ user defined as [24]

$$R_k = \frac{1}{D_k}[a(\theta_{k,1},), a(\theta_{k,2}), \dots, a(\theta_{k,D_k})] \quad (4)$$

Steering vector $a(\theta_{k,i}) \in \zeta^{N \times 1}$ at Angle of Arrival $\theta_{k,i}$ for $k^{th}$ user is given as [24].

$$a(\theta_{k,i}) = [1, e^{(\frac{j2\pi d}{\lambda})\sin\theta_{k,i}}, \dots, e^{(\frac{j2\pi(N-1)d}{\lambda})\sin\theta_{k,i}}]^T, \quad (5)$$

where $d$ and $\lambda$ are distance between antenna element and carrier wavelength respectively. Here, carrier wavelength corresponds to the free space wavelength for 28 GHz. For the rectangle antenna phased array, the steering vector steering matrix defined by [25]

$$a(\theta_{k,i}, \phi_{k,i}) = \\ = vec\{[1, e^{(\frac{j2\pi d}{\lambda})\sin\theta_{k,i}}, \dots, e^{(\frac{j2\pi(N-1)d}{\lambda})\sin\theta_{k,i}}] \otimes \\ \otimes [1, e^{(\frac{j2\pi d}{\lambda})\sin\phi_{k,i}}, \dots \dots, e^{(\frac{j2\pi(N-1)d}{\lambda})\sin\phi_{k,i}}]\}, \quad (6)$$

where $\theta_{k,i}$ and $\phi_{k,i}$ represent elevation AoA and azimuthal AoA, respectively. $vec\{.\}$ represents vectorization of matrix. In massive MIMO system, as the antenna array increase in limited space, mutual coupling also considerable in determination of channel vector redefined as [24]

$$h_k = ZR_k v_k, where\ k = 1,2,3, \dots \dots, K, \quad (7)$$

where steering matrix defined as $R_k \in \zeta^{N \times D_k}$, $D_k$ steering vectors and $v_k \sim \zeta N(0, I_{D_k})$. According to [14, 15], the $Z \in \zeta^{N \times N}$ mutual coupling matrix expressed as

$$Z = (Z_A + Z_L)(\Gamma + Z_L I)^{-1} K, \quad (8)$$

with

$$\Gamma = \begin{bmatrix} Z_A & Z_M & 0 & \dots & 0 \\ Z_A & Z_A & Z_M & \dots & 0 \\ 0 & Z_M & Z_A & \dots & 0 \\ \vdots & \vdots & \vdots & \vdots & \vdots \\ 0 & 0 & \dots & Z_M & Z_A, \end{bmatrix}, \quad (9)$$

where $Z_A$, $Z_L$ and $Z_M$ are antenna mutual impedance between adjacent antenna. Transmit correlation matrix defined as [26]

$$\Sigma_N = E[HH^H] = KZRR^H Z^H, \quad (10)$$

where $R = [R_1, R_2, \dots \dots, R_k]$ is correlation matrix, then mutual coupling channel model $H \sim \zeta N(0, \Sigma_N \otimes I_k)$ helpful in designing of massive MIMO antenna array and effect of antenna spacing on the performance of MIMO system.

## 2.2. Antenna Array

In this article, rectangular array pattern antenna array with $N \times N$ elements are considered where

N = 2, 4, 8, 16 antenna elements. For simplicity, isotropic antenna elements are considered.

An arrangement of 16×16 array is shown in Fig. 2 with aperture size of 85.71 mm and the spacing between adjacent element is 5.357 mm. An array is sub-divided into $N \times 1$ sub-arrays. These sub-arrays are in phased array configuration [4]. Each sub-array forms an element of the MIMO antenna configuration, that is, for a $N \times N$ antenna array composition, there will be N MIMO channels and each channel is comprised of $N \times 1$ phased array antennas [27].

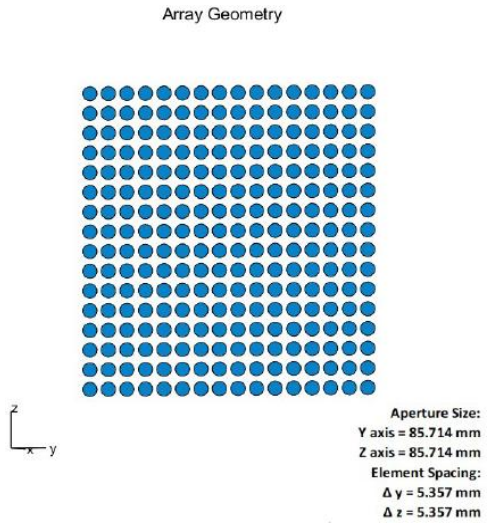



**Fig. 2.** Geometric Pattern rectangular antenna array $N \times M(16 \times 16)$.

A comparison of the radiation characteristics for various array sizes is presented in Table 2. It shows that as the array size increases, the directivity increases significantly. Due to this directive beam pattern, the half power beam width (HPBW) at both the azimuthal and elevation planes decreases. The same is reflected in the radiation patterns illustrated in Fig. 3. The figure further highlights that with increasing array size, the sidelobe levels decrease thereby confining maximum power within a narrow beamwidth.

**Table 2.** Comparative analysis of rectangular array.

| Parameter | Array 2×2 | Array 4×4 | Array 8×8 | Array 16×16 |
|---|---|---|---|---|
| Element Spacing (mm) | 3.357 | 5.357 | 5.357 | 5.357 |
| Directivity (dBi) | 8.63 | 10.09 | 16.51 | 18.90 |
| HPBW(Az) (deg-angle) | 59.92 | 26.30 | 12.00 | 6.36 |
| HPBW(EI) (deg-angle) | 60.00 | 28.00 | 14.00 | 8.00 |

## 3. Hybrid Beamforming

Hybrid beamforming technique is combination of digital beamforming and analog beamforming at its baseband and RF precoding section respectively. Analog beamforming includes a single RF chain but each antenna element is associated to a phase shifter, filter, and weights. Hence, although due to a single RF chain, power consumption is less, in massive MIMO scenario, the requirement of RF components like phase shifters becomes huge thereby increasing the hardware complexity [28].

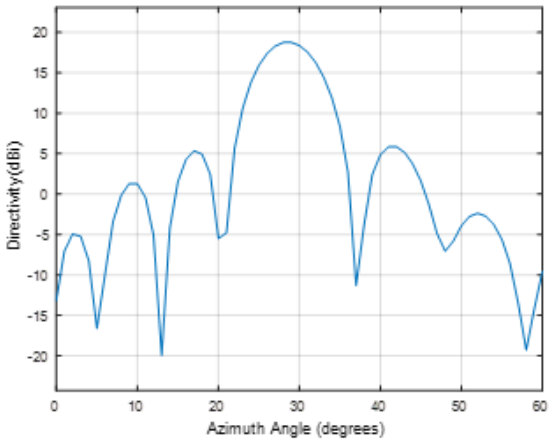



**Fig. 3.** Directivity 16 × 16 antenna array.

The schematic diagrams of the fully-digital beamformer, clustering-based fully connected hybrid beamformer and clustering-based partially connected hybrid beamformer are presented in Fig. 4. The article has already discussed the two stage hybrid precoding technique. In the baseband precoder, signal is adjusted by the precoding weight matrix and in the RF precoder, phase is controlled by the RF weight matrix.

A comparative study of these beamforming techniques is graphically illustrated in Fig. 5 which highlights that Spectral efficiency of optimal digital beamformer and cluster based fully connected approach is higher than the partially connected approach. Fully connected hybrid beamforming structure is outperform as compare to other structure. Furthermore, beamforming flexibility in terms of beam directions and beamwidths is limited. Thus, to reduce the hardware complexity and enhance beamforming flexibility, digital beamforming is introduced where an algorithm-based precoding system is incorporated at the baseband stage. In this technique, each antenna element is associated with a separate RF chain thus increasing the number of RF chains manifold in massive MIMO systems making the beamforming system extremely power hungry. Hybrid beamforming provides a balance between hardware complexity of analog beamforming and power consumption of digital beamforming.

A hybrid beamforming architecture is depicted in Fig. 6. In this technique, two major modifications are incorporated. Firstly, the MIMO array is divided into sub-arrays formed by a cluster of antenna elements. Each sub-array is connected to a phase shifter and associated RF hardware. The phase shift values are controlled by an analog RF precoder. Secondly, each cluster is accompanied by an RF chain connected to a

baseband precoder where digital beamforming is applied by assigning weight vectors to the signals fed to each cluster of antennas [18]. Hence, it can be comprehended that lesser number of RF chains requirement resolves the issue of power consumption faced by digital beamforming. Since the architecture deals with cluster of antenna elements as a unit, the number of RF phase shifters, filters required is also less than the number of antenna elements that simplifies the hardware complexity.

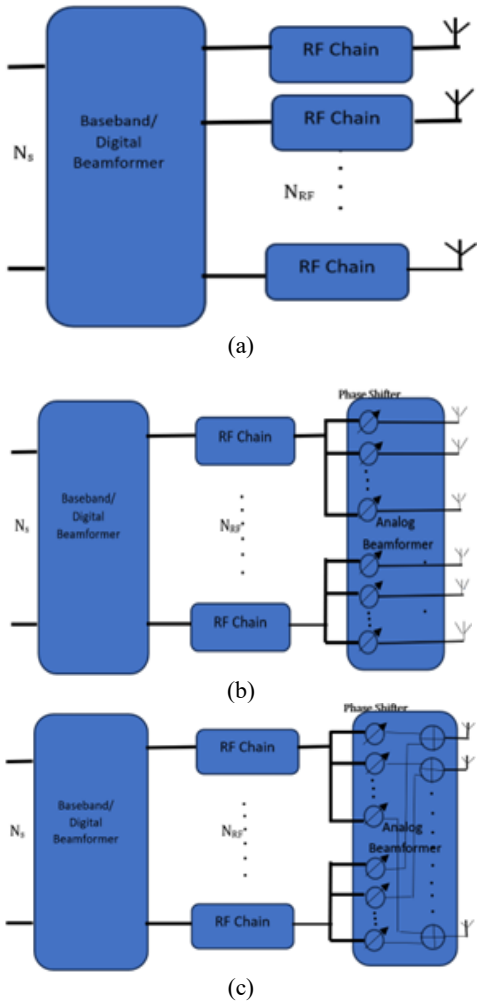



**Fig. 4.** Beamforming Structure: a) Digital beamformer, b) cluster based partially hybrid beamformer, c) Cluster based fully hybrid beamformer.

Multiple data streams sends through the MIMO channel, In order to derive the precoding and combining weight in hybrid beamformer from its channel matrix. Weight are applied in digital baseband significantly enhance the SINR and data rate in MIMO wireless communication [20]. $N_{TRF}$ and $N_{RRF}$ are always less than $N_t$ and $N_r$. Encoded signal $y_k$ transmitted by antenna array that is received at $k^{th}$ user is given by [6, 29].

$$y_k = s_k F_{bb} F_{rf} H_k + \Sigma_{i \neq k}^{K} s_i F_{bb} F_{rf} Hk + n_k, \quad (11)$$

where $n_k$ is i.i.d AWGN noise vector of size $N_r \times 1$ and $n \sim CN(0, \sigma^2)$. $H_k$ is channel matrix for the $k^{th}$ user that can be determined from (3) – (9). $\tilde{y}_k$ is post processing received signal computed at combiner computed as [21].

$$\tilde{y}_k = (s_k F_{bb} F_{rf} H_k + \Sigma_{i \neq k}^{K} s_i F_{bb} F_{rf} H_k + + n_k) W_{rf} W_{bb}, \quad (12)$$

$W_{bb}$ and $W_{rf}$ are the weight matrix at the hybrid beamformer at baseband and RF precoding at combiner section. Performance of the $k_{th}$ user to estimate data stream $\tilde{y}_k$ in term signal to interference noise ratio SINR given by [30]

$$SINR_{j,k} = \frac{|F_{j,k} H_{j,j,k}^{H} W_{j,k}|^2}{\Sigma_{n,l \neq j,k} |F_{n,l} H_{n,j,k}^{H} W_{n,l}|^2 + \sigma^2} \quad (13)$$

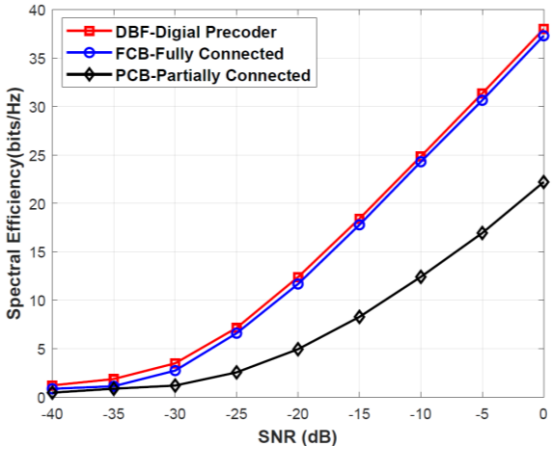



**Fig. 5.** Spectral Efficiency comparison digital beamformer.

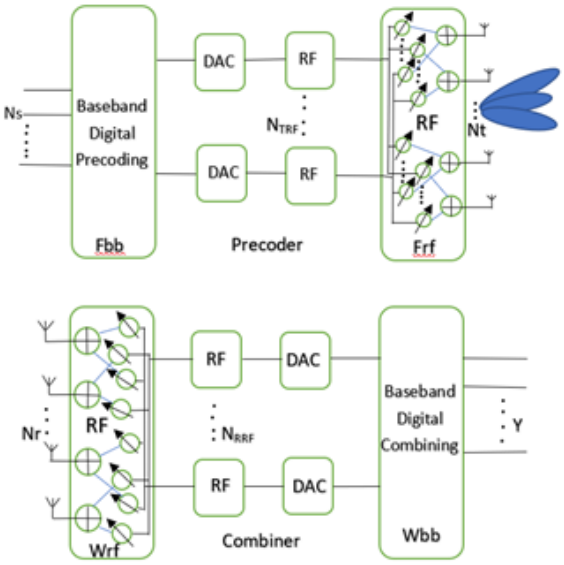



**Fig. 6.** Hybrid beamforming architecture.

Steering beam to the $k^{th}$ user minimized SINR by adjusting the weight vector through efficient

optimization algorithm [29]. In digital beamformer optimal weight can be determined by diagonalization of channel matrix H [29]

$$F \times H \times W \ = \ \Lambda^{-1} H \Lambda, \tag{14}$$

where Λ, eigen vector matrix. $F$ and $W$ are precoding and combining weight matrix of dimension $N_s \times N_t$ and $N_r \times N_s$ respectively.

In this article hybrid beamforming algorithm method Orthogonal Matching Pursuit (OMP), Manifold Optimization and Generalized Eigen Value Decomposition (GEVD) method are implemented for precoder and combiner design. The MMSE based hybrid beamforming formulation and decomposition into subproblem are use from literature [15] and evaluate the performance under different antenna configuration and channel condition. Unlike the previous work, this study foucs on comperative performance analysis in term of spectral efficiency spectral efficiency (SE), mean square Error (MSE), bit error rate (BER), energy efficiency and computational complexity under identical framework.

BER is the important parameter to analyze the efficiency of hybrid beamforming algorithms. In BER performance analysis, the processed received data at $k^{th}$ user equipment from (11) can be re-written as [30]

$$\tilde{y}_k \ = \ s_k F H_k W + \Sigma_{j \neq k}^{K} s_i F H_k W + n_k W \tag{15}$$

Assuming the occurance of symbol error ($s_k \neq \tilde{s}_k$) to the estimated signal, BER can be expressed in terms of SINR as [31], $BER \ = \ Q\sqrt{SINR}$

$$BER_k \ = \ Q\left(\sqrt{\frac{|F_{j,k} H_{j,j,k}^{H} W_{j,k}|^2}{\Sigma_{n,l \neq j,k} |F_{n,l} H_{n,j,k}^{H} W_{n,l}|^2 + \sigma^2}}\right) \tag{16}$$

The formulation of the other two parameters (SE and MSE) is detailed during the discussions on HBF algorithms.

### 3.1. Orthogonal Matching Pursuit

The orthogonal Matching Pursuit (OMP), dictionary based sparse precoding algorithm in mmWave MIMO system [30] is implemented as benchmark scheme for comparative analysis. The presented work, evaluate the performance under identical system assumption and antenna array configuration.

Orthogonal matching pursuit (OMP) algorithm are used as hybrid beamforming algorithm to calculate the precoder solution given as, precoding weight $F = [F_{BB}, F_{RF}]$ and combining weight $W = [W_{BB}, W_{RF}]$ are four set of optimal weight encode the signal and reduce the interference to produce the more steered beam. More the steered beam higher the channel capacity and spectral efficiency [32].

$$R \ = \ log_2 |I - SINR_k| \tag{17}$$

**Algorithm 1. Precoding via Orthogonal Matching Pursuit [30]**

**Input:** $A_t$, $N_t^{RF}$, $N_{cl}$, $N_{ray}$
**Require:** $F_{opt}$
$F_{RF} = EmptyMatrix$
$F_{res} = F_{opt}$
**For** i≤ $N_t^{RF}$ **do**
$\Psi = A_t{}^* F_{res}$ $k = argmax_{l=1 \ldots N_{cl} N_{ray}} (\Psi \Psi^*)$
$F_{RF} = [F_{RF} | A_t^{(k)}]$
$F_{BB} = (F_{RF}^* F_{RF})^{-1} F_{RF}^* F_{RF}$
$F_{res} = \frac{F_{opt} - F_{RF} F_{BB}}{\| F_{opt} - F_{RF}^* F_{RF} \|_F}$
**end for**
$F_{BB} = \sqrt{N_s \frac{F_{BB}}{\| F_{RF} F_{BB} \|_F}}$
**Return** $F_{RF} F_{BB}$

Considering the number of data streams transmitted ($Ns$), SE is calculated as the maximum of R given by

$$R \ = \ log_2 (|I_{N_s} + \\ + \frac{\rho}{N_s} R_n^{-1} W_{BB}^* W_{RF}^* F_{RF} F_{BB} H F_{BB}^* F_{RF}^* W_{RF} W_{BB}|), \tag{18}$$

where $R_n = \sigma_n^2 W_{BB}^* W_{RF}^* W_{RF} W_{BB}$ is the noise covariance matrix. MSE can be estimated for HBF design as [14, 33]

$$MSE \triangleq E \parallel \beta^{-1} y - s \parallel^2, \tag{19}$$

where $s$ is the data stream and $\beta$ is the scaling factor optimize the hybrid beamformer weight, precoder and combiner. The processed data is denoted by $y = W_{BB}^H W_{RF}^H H F_{RF} F_{BB} s + W_{RF}^H W_{BB}^H u$. At the HBF receiver, $W_{RF}$ is the analog combiner weight and $W_{BB}$ is the baseband combiner weight. Received data with additive noise vector $u$ is complex Gaussian distribution at $N_r$ receiver antenna with zero mean and covariance $\sigma^2 I_{N_r}$, i.e. $u\sigma^2 I_{N_r}$, MSE (19) can be expressed as:

$$MSE = E \parallel \beta^{-1} (W_H F s + W_H u - s \parallel^2 = \\ = tr(\beta^{-1} W^H H F F^H H^H W - \beta^{-1} W^H H F \ W + \\ + I_{N_s}) \ - \beta^{-1} F^H H^H W + \sigma^2 \beta^{-2} W^H, \tag{20}$$

where $F$ and $W$ are baseband and combiner weight matrices over all beamformer. $F_{RF}$ and $W_{RF}$ are analog beamformer weights to adjust the phase. Analog beamformer should satisfy the constant modulus constraints of the phase shifter, defined as $|[F_{RF}]_{i,j}| = 1$, for $i = 1, \ldots, N_t$ and $j = 1, \ldots, N_{RF}$, and $|[W_{RF}]_{i,j}| = 1$, for $i = 1, \ldots, N_t$ and $j = 1, \ldots, N_{RF}$. MSE expression formulating the HBF optimization problem as

$$\min_{F_{RF},F_B,W_{RF},W_B} \quad MSE, \tag{21}$$

$$\text{subject to:} \quad \| F \|_B^2 \leq 1, \forall_{i,j}, \tag{22}$$

$$|[W_{RF}]_{m,l}|^2 = 1, \forall_{m,l} \tag{23}$$

**Algorithm 2. Combining via Orthogonal Matching Pursuit [30]**

**Input:** $A_r$, $N_t^{RF}$, $N_{cl}$, $N_{ray}$
**Require:** $W_{opt}$
$W_{RF} = EmptyMatrix$
$W_{res} = W_{opt}$
**For** i$\leq N_r^{RF}$ do
$\Psi = A_r^* E[yy^*] W_{res}$
$k = argmax_{l=1\ldots N_{cl}N_{ray}} (\Psi\Psi^*)_{l,l}$
$W_{RF} = [W_{RF} | A_r^{(k)}]$
$W_{BB} = (W_{RF}^* E[yy_*] W_{RF})^{-1} W_{RF}^* E[yy_*] W_{opt}$
$W_{res} = \frac{W_{opt} - W_{RF} W_{BB}}{\|W_{opt} - W_{RF}^* W_{opt}\|_F}$
**End for**
$W_{BB} = \sqrt{N_s} \frac{W_{BB}}{\|W_{RF} W_{BB}\|_F}$
**Return** $W_{RF} W_{BB}$

## 3.2. Manifold Optimization Algorithm

The Manifold optimization technique adopted in this work to solve the constrained hybrid beamforming problem directly under MMSE criteria [15]. The presented article uses these hybrid beamforming formulation for consider the antenna array and RF chain configuration.

Manifold hybrid beamforming algorithm optimize the precoder and combiner divide original problem into subproblem. MSE optimization given in equation (21) to calculate precoding matrix $F_{BB}$and scaling factor $\beta$ [34].

$$\beta = (tr(F_{RF} F_{BB} F_{BB}^H F_{RF}^H))^{-\frac{1}{2}}, \tag{24}$$

and

$$F_{BB} = (F_{RF}^H H_1 H_1^H F_{RF} + \sigma^2 \omega F_{RF^H F_{RF}})^{-1} F_{RF} H_1 \tag{25}$$

Conjugate gradient function equation (26) optimized RF precoder by minimized the objective to find optimal solution to maximize the transit power level [29].

$$\nabla J(F_{RF}) = \frac{1}{\sigma_2 \omega} (F_{RF} \left(F_{RF}^H F_{RF}\right)^{-1} - I_{N_s}) \times \times H_1 P^{-2} H_1^H F_{RF} (F_{RF}^H F_{RF})^{-1} \tag{26}$$

**Algorithm 3. Precoding Via MO- HBF**

**Input:** $H_1$, $\sigma^2$, $\omega$, $\alpha$
**Require:** $F_{RF}, F_{BB}, \beta$
Set i=0, initialize $F_{RF,i}$;
**For** i$\leq N_{max}$ do
$\nabla J(F_{RF}) = \frac{1}{\sigma_2 \omega} (F_{RF} (F_{RF}^H F_{RF})^{-1} - I_{N_s}) \times$
$\times H_1 P^{-2} H_1^H F_{RF} (F_{RF}^H F_{RF})^{-1}$
$F_{RF,i+1} = F_{RF,i} - \alpha \nabla J(F_{RF})$
$i \leftarrow i + 1$
**End for**
$\beta = (tr(F_{RF} F_{BB} F_{BB}^H F_{RF}^H))^{\frac{-1}{2}}$
$F_{BB} = (F_{RF}^H H_1 H_1^H F_{RF} + \sigma^2 \omega F_{RF^H F_{RF}})^{-1} F_{RF} H_1$
**Return** $F_{RF} F_{BB}$

Hybrid receiver combiner is designed after updating the precoding weight matrices according to scaling factor $\beta$. The optimization problem can rewrite at hybrid receiver combiner as [34, 35]

$$\min_{W_{RF},W_B} tr(W_H H_2 H_2^H W - W^H H_2 - H_2^H W + \sigma^2 \beta - 2W^H W + I_{N_s}), \tag{27}$$

$$\text{subject to:} \ |[W_{RF}]_{i,j}| = 1, \forall_{i,j}, \tag{28}$$

where $H_2 \triangleq H F_{RF} F_{BB}$ and $W \triangleq W_{RF} W_{BB}$. Objective function differentiating $W_B$ and setting the result to zero, optimal $W_B$ is obtained as

$$W_B = (W_{RF}^H H_2 H_2^H W_{RF} + \sigma^2 \beta^{-2} W_{RF^H W_{RF}})^{-1} W_{RF} H_2 \tag{29}$$

RF combiner optimization problem can be reduced to the following optimization of $W_{RF}$ as

$$\min_{W_{RF}} J(W_{RF}) \triangleq tr(I_{N_s} + \sigma^2 \beta^{-2} H_2^2 W_{RF} \times \times (W_{RF}^H W_{RF})^{-1} W_{RF}^H H_2)^{-1}, \tag{30}$$

$$\text{subject to:} \ |[W_{RF}]_{i,j}| = 1, \forall_{i,j} \tag{31}$$

MO-HBF is directly applied and implemented in the precoder matrix.

## 3.3. Generalized Eigen Value Decomposition

The generalized eigenvalue decomposition (GEVD) based hybrid beamforming framework proposed in Lin et al. [15] implemented to evaluate the performance under unified framework. The hybrid beamforming algorthim structure follows the MMSE reformulation and columnn wise optimization strategy match with antenna array configuration and simulation enviornment.

The gradient based algorithm optimizes the analog precoding weight matrix $F_{RF}$. The complexity of GEVD algorithm dependent on number of iterations, which is trade-off with suprior performance of spectral efficiency. According to [8, 36] for MIMO system, $F_{RF}^H F_{RF} \approx N_t I_{N_{RF}}$ different data streams are orthogonal to each for optimized analog beamforming, with this approximation, is MSE defined as:

$$J(F_{RF}) \approx tr(I_{N_s} + \frac{1}{\sigma^2 \omega Nt} H_1^H F_{RF} F_{RF}^H H_1)^{-1}) \quad (32)$$

Precoding matrix is optimized column by column, $V_m$ is sub matrix of $F_{RF}$ after the optimization of the $m_{th}$ column. Furthermore, $A_m \triangleq I_{N_s} + \frac{1}{\sigma^2 \omega Nt} H_1^H V_m V_m^H H_1$. Using the identity $(A+B)^{-1} = A^{-1} - \frac{A^{-1}BA^{-1}}{1+tr(A^{-1}B)}$, the MSE can be expressed as [37]:

$$J(F_{RF}) \approx tr(A_m)^{-1} - \\ - \frac{tr\left(\frac{1}{\sigma^2 \omega Nt} A_m^{-1} H_1^H v_m v_m^H H_1 A_m^{-1}\right)}{1+tr\left(\frac{1}{\sigma^2 \omega Nt} A_m^{-1} H_1^H v_m v_m^H H_1\right)} = tr(A_m^{-1}) - \\ - \frac{v_m^H U_m v_m}{v_m^H W_m v_m}, \quad (33)$$

where $U_m \triangleq \frac{1}{\sigma^2 \omega Nt} H_1 A_m^{-2} H_1^H$ and $W_m \triangleq \frac{1}{N_t} + \frac{1}{\sigma^2 \omega Nt} H_1 A_m^{-2} H_1^H$ are both Hermitian matrices. In the equation (33), MSE is divided into two terms, $V_m$ and $v_m$. By keeping the $V_m$ fixed, $J(F_{RF})$ is the function of $v_m$ in second term in (33). The optimal $v_m$ maximizes the second term and minimizes the whole term in equation (33). Minimizing the MSE in equation (33) is accomplished by maximizing the generalized eigen value between the $U_m$ and $W_m$, obtained by GEVD operation. Phase extraction operations, extract the phase of antenna element in each column. The steps for the whole $V_{RF}$ matrix are repeat until the stop condition is satisfied.

**Algorithm 4. GEVD- Based Hybrid Beamforming Alogorithm [15]**

**Input:** $H_1$, $\sigma^2$, $\omega$,
**Input:** $H_1$, $\sigma^2$, $\omega$,
**Require:** $F_{RF}, F_{BB}, \beta$
Set $i = 0$, Initialize $F_{RF,i}$;
**For** $1 \leq m \leq N_{RF}$ **do**
Evaluate $A_m, U_m, W_m$
$A_m \triangleq I_{N_s} + \frac{1}{\sigma^2 \omega Nt} H_1^H V_m V_m^H H_1$.
$U_m \triangleq \frac{1}{\sigma^2 \omega Nt} H_1 A_m^{-2} H_1^H$
$W_m \triangleq \frac{1}{N_t} + \frac{1}{\sigma^2 \omega Nt} H_1 A_m^{-2} H_1^H$
Evaluate the maximum generalized eigenvector $z$ of $U_m$ and $W_m$
Set $v_{m,i}$ =exp(J∠ (z), where $\angle(z)$ extract the phase of each element of $z$
$i \leftarrow i + 1$
**End for**
Compute $\beta$ and $F_{BB}$
$\beta = (tr(F_{RF} F_{BB} F_{BB}^H F_{RF}^H))^{\frac{-1}{2}}$
$F_{BB} = (F_{RF}^H H_1 H_1^H F_{RF} + \sigma^2 \omega F_{RF^H F_{RF}})^{-1} F_{RF} H_1$
**Return** $F_{RF} F_{BB}$

The overall GEVD HBF algorithm optimizes the precoding analog matrix. By fix the precoding matrices $F_{RF}$, $F_B$ and scaling factor $\beta$, the optimization problem rewrite for hybrid receiver combiner [14, 32]

$$\min_{W_{RF} W_B} tr(W_{RF}^H W_B^H H F_{RF} F_B F_B^H F_{RF}^H H^H W_{RF} W_B - \\ - W_{RF}^H W_B^H H F_{RF} F_B - H_2^H W_{RF} W_B + \\ + \sigma^2 \beta^{-2} W_{RF}^H W_B^H W_{RF} W_B + I_{N_s}), \quad (34)$$

$$\text{subject to } |[W_{RF}]_{i,j}| = 1, \forall_{i,j} \quad (35)$$

Objective function differentiating with respect to $W_B$ in in equation (34) and setting to zero, to find the resultant optimal combiner in equation defined as [14]

$$W_B = (W_{RF}^H H F_{RF} F_B F_B^H H^H W_{RF} + \\ + \sigma^2 \beta^{-2} W_{RF}^H W_{RF})^{-1} W_{RF}^H H F_{RF} F_B F_B^H F_{RF}^H H^H \quad (36)$$

RF combiner matrix $W_{RF}$, after optimization reduce to the following optimization problem

$$\min_{W_{RF}} J(W_{RF}) \triangleq tr((I_{N_s} + \sigma^2 \beta^{-2} F_B^H F_{RF}^H H_H W_{RF}) \times \\ \times (W_{RF}^H W_{RF})^{-1} W_{RF}^H H F_{RF} F_B)^{-1} \quad (37)$$

$$\text{subject to } |[W_{RF}]_{i,j}| = 1, \forall_{i,j} \quad (38)$$

GEVD -HBF algorithm is implemented directly to optimize the hybrid combiner.

## 3.4. Broadband Scenario

The hybrid beamforming algorithm can be extended to the broadband mmWave system in which the OFDM technology is to be implemented to avoid the channel frequency selectivity [38, 39]. The work follows the wideband OFDM MMSE framework [39] 40]. This section include the theoretical extension and future research extension.

Precoder weight matrix optimization is required for all the subcarriers. MSE for the $k^{th}$ subcarrier is defined by [35, 40]

$$MSE_k = E(\| s_k - \beta^{-1} y_k \|^2), \quad (39)$$

where, $\beta_k$ is scaling factor the $k^{th}$ subcarrier, $S_k$ is transmitted symbol and $y_k$ is received power at the $k^{th}$ subcarrier. Optimization objective for broadband scenario can be defined as [36]

$$\min_{F_{B,k}, F_{RF}, W_{B,k}, W_{RF}} \Sigma_{k=0}^{N-1} MSE_k, \quad (40)$$

$$\text{subject to } \| F_k \|^2 \leq 1, \quad (41)$$

$$|[F_{RF}]_{i,j}|^2 = 1, \forall_{i,j}, \quad (42)$$

$$|[W_{RF}]_{m,l}|^2 = 1, \forall_{m,l}, \quad (43)$$

Maximization of the spectral efficiency for the broadband WMMSE HBF optimization objective formulated as [36]

$$\min_{F_k, W_k, \beta_k, \Delta_k} \Sigma_{k=0}^{N-1} (tr(\Delta_k T_k) - log|\Delta_k|, \quad (44)$$

$$\text{subject to } \| F_k \|^2 \leq 1, \quad (45)$$

$$|[F_{RF}]_{i,j}|^2 = 1, \forall_{i,j}, \quad (46)$$

$$|[W_{RF}]_{m,l}|^2 = 1, \forall_{m,l}, \quad (47)$$

where, $T_k$ and $\Delta_k$ represent MSE and weight for the $k^{th}$ sub carrier respectively. When the objective function narrowband scenario is taken into consideration, it is seen that only constant weight matrix $\Delta_k$ is replaced by $I_{N_s}$.

### 3.5. Computational Complexity Analysis

In this section we discuss the computation complexity of the hybrid beamforming algorithm, focusing on complex multiplication. Both the transmit precoding and receiving combining subproblems follow unified procedure. Hybrid beamforming iteratively selects the best transmit antennas based on channel characteristics. The complexity of this step depends on the number of RF chains per sub-array ($N_{RF}$) and the number of data streams ($N_s$) [31]. In orthogonal Matching Pursuit (OMP), complexity primarily depends on the antenna ($A_t$) and optimal beamforming matrices ($F_{opt}$). With a loop iteration of ($N_{RF}$), the overall complexity is $O(N_{RF}(N_t \times N_{cl} \times N_{ray} + N_{RF}^3))$ [41]. In Manifold Optimization (MO) precoder maximize the signal power and complexities lies in the conjugate gradient function, contributing $O(N_{RF}^3 + N_t^3 + N_t^2 \times N_{RF} + N_{RF}^2 \times N_t)$ per iteration, resulting in an overall complexity of $O(N_{max}(N_{RF}^3 + N_t^3 + N_t^2 \times N_{RF} + N_{RF}^2 \times N_t)$. GEVD performs a decomposition of the channel matrix into its eigen vectors and eigen values. The computational complexity of this step depends on the size of the channel matrix. Generalized Eigenvalue decomposition (GEVD) involve computing $U_m$ and $W_m$, contributing $O(N_s^3 + N_t \times N_s^2 + N_t^2 \times N_s)$ per iteration. The overall complexity is $O(N_{RF}(N_s^2 + N_t \times N_s^2 + N_t^2 \times N_s) + N_{RF}^3 + N_{RF}^2 \times N_t))$. The comparison of the computational complexity of the all-beamforming algorithms is given below Table 3.

**Table 3.** Comparative Complexity Analysis of HBF Algorithms.

| HBF Algorithm | Computational Complexity |
|---|---|
| OMP | $O(N_{RF}(N_t \times N_{cl} \times N_{ray} + N_{RF}^3))$ |
| MO | $O(N_{max}(N_{RF}^3 + N_t^3 + N_t^2 \times \times N_{RF} + N_{RF}^2 \times N_t)$ |
| GEVD | $O(N_{RF}(N_s^2 + N_t \times N_s^2 + N_t^2 \times \times N_s) + N_{RF}^3 + N_{RF}^2 \times N_t))$ |

For $N_{RF} = 4, N_s = 4$ and $N_t = 64$ computational complexity $O(256N_{cl}N_{ray} + 256)$ for precoding via OMP HBF, higher complexity depend on $N_{cl}$ and $N_{rayl}$. OMP HBF algorithm is relatively simple to implement, making it suitable for real-time applications and systems with hardware constraints. Complexity calculate for given parameter in manifold hybrid beamforming is $O(N_{max}(279616))$. It shows complexity dependency on $N_{max}$, which is significantly higher complexity. MO HBF algorithm can achieve improved beamforming accuracy by jointly optimizing both analog and digital precoders and providing potential benefits for interference management. GEVD provides the optimal solution for maximizing the received signal-to-noise ratio. While GEVD offers higher spectral efficiency and complexity for GEVD is $O(70976)$.

## 4. Simulation Results

In this section, simulation evaluate the performance of the described HBF algorithms through Monte Carlo simulation in a mmWave massive MIMO communication enviornment operating at carrier frequency of 28 GHz. The narrowband channel model is designed with cluster size $N_C = 6$, number of the rays $N_{Ray} = 8$ per cluster and scattered channel is $N_{Ray} \times N_C$. The transmitter and reciever equiped with uniform rectuagular array (URAs) with antenna element sapcing $\frac{\lambda}{2}$ = 5.357 mm. It is assumed that angle of arrival and departure distributed with angular spread 10 degree with in mean cluster angle in $[0,2\pi]$. Uniform rectangular array (URA) subdivided in uniform in Uniform linear array. The hybrid beamforming architecture employs number of RF chain $N_{RF} = 4$ and the number of data stream $N_s$ varies from 1 to 4, subject to constraint $N_s \leq N_{RF}$. The constatnt modulus phase shifter assumed analog beamforming network and it satisfy unit magnitude constraint. The simulation results obtained with 400 Motnte Carlo realization. Simulation provided to implement the HBF optimization algorithm at precoder and combiner stages with different size array as $2 \times 2, 4 \times 4, 8 \times 8, 16 \times 16$ and length of data stream in QPSK modulated at baseband precoder. The simulation section evaluate the spectral effciency, MSE, BER and energy efficiency by implementation of persented HBF algorithms in common framework and parameter in given parameter Table 4.

**Table 4.** List of Parameter.

| Parameter | Value |
|---|---|
| Carrier Frequency | 28 GHz |
| Number of Cluster ($N_c$) | 6 |
| Rays per Clusters ($N_{ray}$) | 8 |
| Modulation Scheme | QPSK |
| Data Stream ($N_s$) | 1-4 |
| Antenna Arrays | 2×2, 4×4, 8×8, 16×16 |
| Antenna Spacing | $\frac{\lambda}{2}$ = 5.357 mm |
| SNR Range | -40 dB - 0 dB |
| Phase Shifter | Constant Modulus |

### 4.1. Spectral Efficiency Performance

Fig. 7 and Fig. 8 graphically depict the spectral efficiency achieved by the beamforming algorithms.

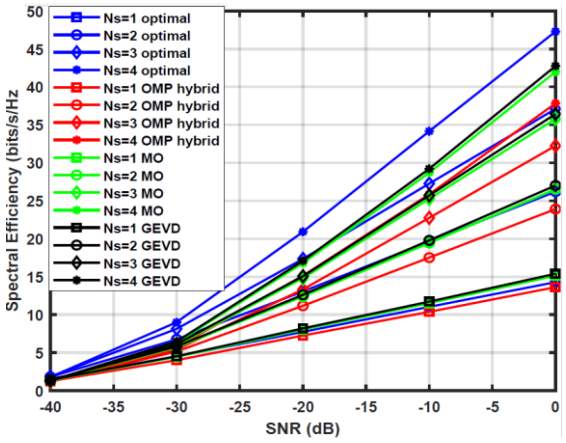



**Fig. 7.** Spectral Efficiency at different length DataStream, Array size 16 × 16.

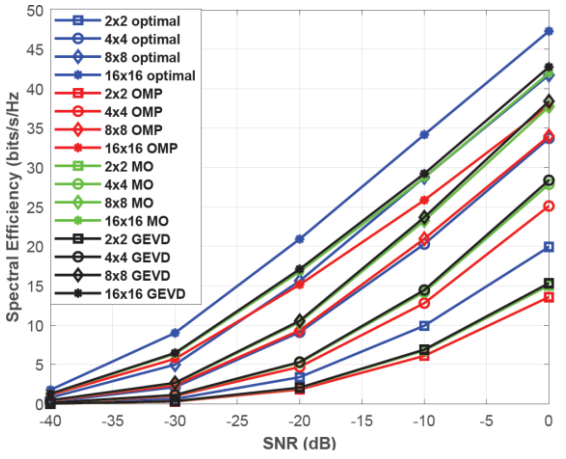



**Fig. 8.** Spectral Efficiency at different Array Size, DataStream length $Ns = 4$.

From Fig. 7, it is observed that when the data stream length ($N_s$) is less GEVD and MO algorithms give slightly better performance than optimal algorithm with GEVD being marginally improved than MO. As $N_S$ increases to 4 and beyond, performance of optimal algorithm exceeds the others. Fig. 8 highlights that with different antenna array size the optimal algorithm gives overwhelmingly better result than any HBF algorithm. For HBF algorithms, GEVD and MO have almost similar performances.

It is also observed that as the array size is increasing, the difference between full digital beamforming (optimal) and the HBF algorithms (GEVD and MO) is decreasing steadily thus indicating that for extremely large massive MIMO cases, GEVD and MO will give almost similar spectral efficiency as optimal with GEVD being more advantageous due to its cost effectiveness. In all the cases, OMP algorithm lags behind thereby concluding that OMP is not a suitable HBF technique where spectral efficiency is the primary objective.

Table 5 tabulates the spectral efficiency values at 0 dB, to comprehend the performance of the HBF algorithms numerically. When array size is less, GEVD HBF is comparable to optimal beamforming. As array size increases, with increasing number of data streams, the performance of GEVD and MO become comparable to optimal beamforming. MO surpasses GEVD when data stream is less.

**Table 5.** Spectral Efficiency (bits/Hz) Comparison (SNR = 0 dB).

| Beamforming | $N_S$ | Array 2×2 | Array 4×4 | Array 8×8 | Array 16×16 |
|---|---|---|---|---|---|
| Optimal (Full Digital) | 1 | 10 | 11 | 13 | 26 |
| | 2 | 16 | 20 | 23 | 26 |
| | 3 | 17 | 26 | 32 | 37 |
| | 4 | 17 | 30 | 40 | 47 |
| OMP HBF | 1 | 10 | 11 | 13 | 14 |
| | 2 | 14 | 18 | 22 | 24 |
| | 3 | 14 | 23 | 28 | 31 |
| | 4 | 15 | 25 | 23 | 37 |
| MO HBF | 1 | 10 | 11 | 13 | 15 |
| | 2 | 12 | 20 | 24 | 36 |
| | 3 | 13 | 25 | 32 | 36 |
| | 4 | 15 | 28 | 37 | 42 |
| GEVD HBF | 1 | 11 | 12 | 14 | 17 |
| | 2 | 15 | 20 | 27 | 27 |
| | 3 | 15 | 26 | 32 | 37 |
| | 4 | 16 | 29 | 38 | 43 |

### 4.2. Mean Square Error (MSE) Performance

MSE is another performance parameter that evaluates the 5G test bench performance after implementation of HBF algorithm. For transmitted RF signal through scattered channel $H$, while taking into account noisy channel and interference from adjacent user, MSE is formulated for various HBF algorithms as discussed in Section 3 which is mainly dependent on the channel condition, array dimension and size. MSE is evaluated for the 20 iterations and SNR from -40 dB to 0 dB.

Fig. 9 exhibits the MSE performance for the HBF algorithms for various MIMO array sizes. With increase in array size, the directional gain increases due to larger number of subarray selection. Keeping channel condition fixed, increase in directional gain lowers the interference from adjacent users that reduces the MSE. As a result, for all the algorithms, MSE decreases with increase in array size although the differences become small with increased SNR. Among the HBF algorithms, GEVD has minimum MSE due its control ability at the RF precoder level in transmitter section. It is observed that MSE for OMP algorithm tends to catch up MO algorithm as array size increases.

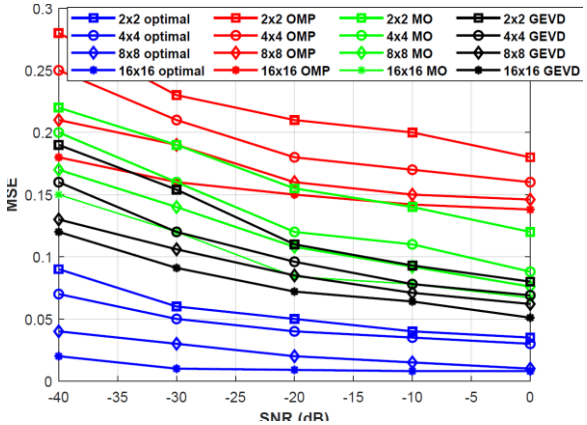



**Fig. 9**. MSE performance HBF algorithms at different array size.

MSE performance is evaluated with different length of data stream transmitted through the precoder circuit and presented in Fig. 10. It is seen that for higher data stream, as SNR increases, the MSE flattens and approaches constant value for GEVD and optimal beamforming techniques. GEVD is still the better candidate among the HBF algorithms. For higher data streams, with increasing SNR, the MSE decreases drastically for OMP algorithm and almost exceeds MO performance at near 0 dB SNR value.

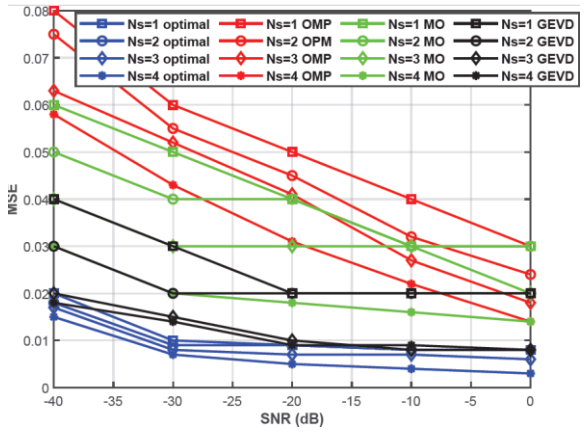



**Fig. 10.** MSE performance with different Data Stream.

## 4.3. Bit Error Rate (BER) Performance

BER performance of the beamforming algorithms has been evaluated based on (16). Fig. 11 shows the BER performance based on the length of data stream. The figure indicate, in noisy condition GEVD and MO HBF perform slightly improved BER in certain simulation realization such as finite Monte Carlo simulation and MMSE based optimization framework. As the SNR increase, fully digital beamforming remain upperbound benchmark of the perormance.

Furthermore, with an increase in the length of data stream, the BER decreases at low SNR values for all the beamforming techniques. As SNR increases, the BER decreases significantly and the length of data stream does not play any role to affect the BER. Overall, OMP algorithm has the worst performance.

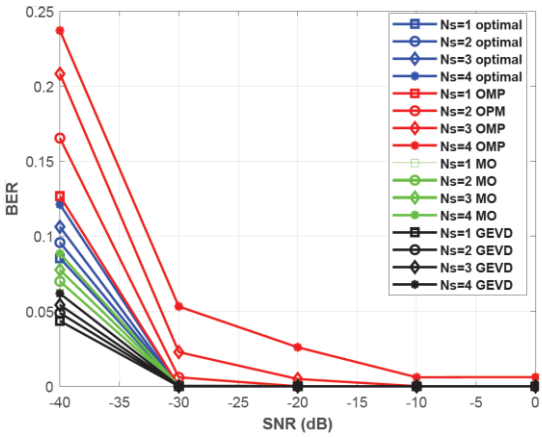



**Fig. 11.** BER at different length of Data Stream, Array Size 16×16.

Fig. 12 exhibits the effect of array size on the BER performance of the beamforming algorithms. For any particular array size OMP HBF exbhits highest BER, where MO HBF and GEVD HBF achieve BER peroformance close to Optimal digital beamforming. Among all the hybrid beamforming hybrid beamforming, the GEVD HBF consistently perform better BER with increase the SNR. Energy efficiency gains in sub-array precoding depend on various factors, including system design, specific algorithms used, and environmental conditions. Therefore, proper optimization and careful consideration of the system parameters are crucial to achieving maximum energy efficiency benefits.

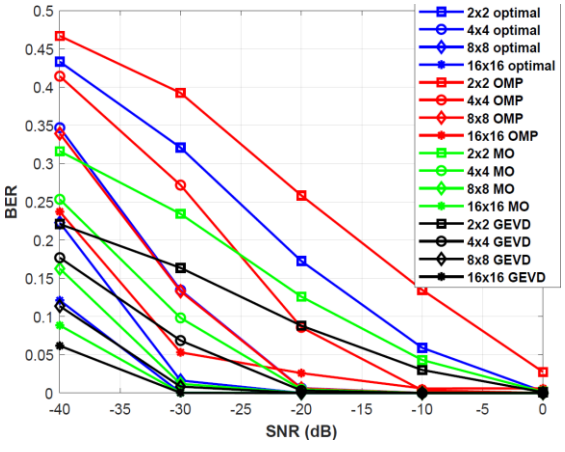



**Fig. 12.** BER at different Array Size, $Ns = 44.4$ Energy Efficiency Performance.

In the present work, the transmitter power $PT = 1\,W$ is considered. The energy efficiency is defined as $\eta = R/PT$, where R is achievable rate

[37]. The number of RF chain $N_{RF}$ and number of receiver antenna Nr are 4 and 64 respectively. Fig. 13 shows the energy efficiency performance with the number of transmitter antennas (Nt). It indicates that the energy efficiency increases with increase in $N_t$ with a tendency to flatten out as $N_t$ increases without bound. GEVD and MO HBF algorithms have almost identical performance while OMP HBF has the poorest performance. Fig. 14 exhibits energy efficiency performance with respect to SNR for various array configuration which reveals that for lower configuration energy efficicny GEVD HBF and MO HBF outperform optimal digital precoder due to reduced number RF chain and assoiciated hardware power consumtion.

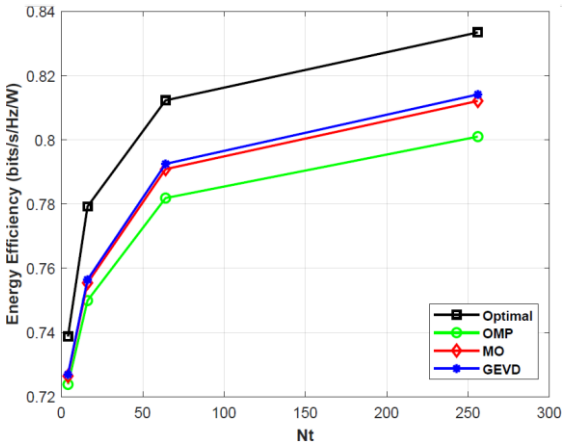



**Fig. 13.** Energy Efficiency Vs $N_t$.

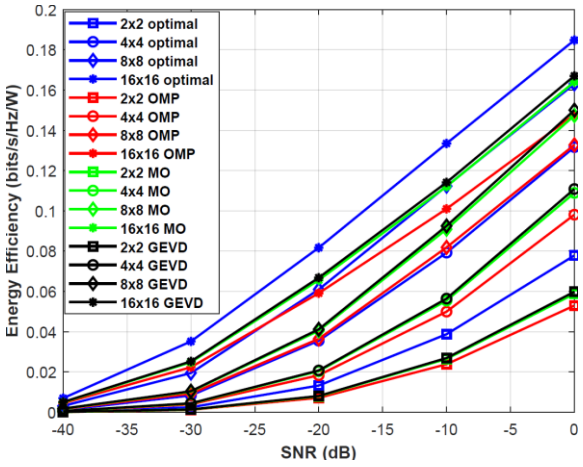



**Fig. 14.** Energy Efficiency Vs SNR (Ns = 1,2,3,4).

The performance of the presented HBF algorithms in the manuscript are compared with other HBF algorithms found in literature in terms of spectral efficiency (SE), mean square error (MSE) and bit error rate (BER). The comparison table is given in Table 6. From the table, it is revealed that with comparatively lesser number of antenna array elements and RF chains ($N_{RF}$), better performance is achieved by the presented HBF algorithms relative to the other HBF algorithms found in literature.

**Table 6.** Comparison of presented HBF algorithms with other reported HBF algorithms.

| Cite | Methodology | Parameter | SE | MSE | BER |
|---|---|---|---|---|---|
| [42] | Zero forcing beamforming algorithm | $N_{RF} = 8$, Ns = 4 | 32 | 0.24 | $10^{-1}$ |
| [43] | MMSE based Rate Balancing Hybrid precoding | $N_{RF} = 3$, Ns = 2 | 20 | ... | ... |
| [44] | Constrained-SVD based hybrid beamforming | $N_{RF} = 4$, Ns = 4 | 28 | ... | $10^{-1}$ |
| [45] | GMD based hybrid beamforming | $N_{RF} = 3$, Ns = 3 | 14 | 0.16 | $10^{-2}$ |
| [46] | Gram-Schmidt based greedy algorithm | $N_{RF} = 3$, Ns = 2 | 10 | 0.21 | $10^{-1}$ |
| [24] | Eigen-Beamforming | $N_{RF} = 10$, Ns = 4 | 35 | 0.12 | $10^{-2}$ |
| Present work | Orthogonal Matching Pursuit | $N_{RF} = 4$, Ns = 4 | 37 | 0.14 | 0.0276 |
| Present work | Manifold Optimization | $N_{RF} = 4$, Ns = 4 | 42 | 0.067 | 0.0015 |
| Present work | GEVD HBF Algorithm | $N_{RF} = 4$, Ns = 4 | 43 | 0.051 | 0.0011 |

## 5. Conclusion

This article proposed HBF technique in mm-wave massive MIMO antenna configuration. 4, 16, 64 and 256 isotropic antenna elements have been considered in rectangular array pattern to configure the massive MIMO arrangement. $N \times 1$ elements have been clustered together to form a phased array antenna. N rows of phased array antennas form the N-ports of the MIMO antenna. It has been demonstrated that as the number of antenna elements increases in the phased array, directivity gain increases while beamwidth decreases and number of side lobes also increases. In order to minimize inter-element interference and increase channel capacity, HBF technique has been employed with optimizing the precoding weights at the baseband and combining weights at the RF sections. The various HBF algorithms used are MO, OMP and GEVD which are compared with full digital beamforming algorithm in terms of SE, MSE and BER. It has been demonstrated that with increased data streams, all the algorithms perform very well even under low SINR condition. Although digital beamforming repersents the theoretical performance upperbound, the simulation resuts with GEVD HBF and MO HBF algorithm better BER performce close to digital beamforming under considered MMSE based framework and simulation assumption. The overall, GEVD provide suprior BER, MSE performance and maintaining lower complexity requirement than manifold optimization technique. It

is most favourable trade-off between the performance and complexity cost. The investigations indicate that for large number of antenna elements, SE for MO and GEVD become comparable to full digital beamforming. The analysis and performance evaluation provided in this work will help as guidance to judge the best suited HBF optimization technique to be used for any particular mm-wave massive MIMO scenario.

## References


[1]. I. Ahmed, H. Khammari, A. Shahid, A. Musa, et al., A survey on hybrid beamforming techniques in 5G: Architecture and system model perspectives, *IEEE Communications Surveys & Tutorials*, Vol. 20, Issue 4, 2018, pp. 3060-3097.

[2]. E. Ali, M. Ismail, R. Nordin, N. F. Abdulah, Beamforming techniques for massive MIMO systems in 5G: Overview, classification, and trends for future research, *Frontiers of Information Technology & Electronic Engineering*, Vol. 18, Issue 6, 2017, pp. 753-772.

[3]. R. N. Revankar, A. N. Kashyap, S. Shravan, M. C. Nithya Shree, et al., Hybrid beamforming in 5G massive MIMO, in *Proceedings of the International Conference on the Confluence of Advancements in Robotics, Vision and Interdisciplinary Technology Management (IC-RVITM)*, 2023, pp. 1-6.

[4]. S. I. Farghaly, M. M. Fouda, M. M. Emara, Beamforming of transmit antennas using grey wolf optimization and L2-norm for performance enhancement of beyond 5G communications, *IEEE Open Journal of Antennas and Propagation*, Vol. 5, 2024, pp. 1-12.

[5]. A. Mahmud, A. Ali, R. S. Dhar, S. G. Razavipour, et al., Scanning voltage microscopy for emerging electronic and photonic devices: Integrating nanotips with a single atom end for SVM, *IEEE Nanotechnology Magazine*, Vol. 11, Issue 1, 2017, pp. 4-11.

[6]. A. Garcia-Rodriguez, V. Venkateswaran, P. Rulikowski, C. Masouros, Hybrid analog-digital precoding revisited under realistic RF modeling, *IEEE Wireless Communications Letters*, Vol. 5, Issue 5, 2016, pp. 528-531.

[7]. I. Chatterjee, J. Singh, S. Srivastava, A. K. Jagannatham, Frequency selective hybrid beamforming and optimal power loading for multiuser millimeter-wave cognitive radio networks, *IEEE Access*, Vol. 11, 2023, pp. 116310-116326.

[8]. L. Jiang, H. Jafarkhani, Multi-user analog beamforming in millimeter-wave MIMO systems based on path angle information, *IEEE Transactions on Wireless Communications*, Vol. 18, Issue 1, 2019, pp. 608-619.

[9]. R. S. Dhar, L. Li, H. Ye, X. Wang, et al., Nanoscopically resolved dynamic charge-carrier distribution in operating interband cascade lasers, *Laser & Photonics Reviews*, Vol. 9, Issue 2, 2015, pp. 224-230.

[10]. L. Dai, X. Gao, Z. Wang, Energy-efficient hybrid precoding based on successive interference cancellation for millimeter-wave massive MIMO systems, in *Proceedings of the Radio and Antenna Days of the Indian Ocean (RADIO)*, 2015, pp. 1-2.

[11]. F. Sohrabi, W. Yu, Hybrid digital and analog beamforming design for large-scale antenna arrays, *IEEE Journal of Selected Topics in Signal Processing*, Vol. 10, Issue 3, 2016, pp. 501-513.

[12]. K. Zheng, S. Ou, X. Yin, et al., Massive MIMO channel models: A survey, *International Journal of Antennas and Propagation*, Vol. 2014, 2014, 848071.

[13]. H.-H. Tseng, Y.-F. Chen, S.-M. Tseng, Hybrid beamforming and resource allocation designs for mmWave multi-user massive MIMO-OFDM systems on uplink, *IEEE Access*, Vol. 11, 2023, pp. 133070-133085.

[14]. E. G. Larsson, O. Edfors, F. Tufvesson, T. L. Marzetta, Massive MIMO for next generation wireless systems, *IEEE Communications Magazine*, Vol. 52, Issue 2, 2014, pp. 186-195.

[15]. T. Lin, J. Cong, Y. Zhu, J. Zhang, et al., Hybrid beamforming for millimeter-wave systems using the MMSE criterion, *IEEE Transactions on Communications*, Vol. 67, Issue 5, 2019, pp. 3693-3708.

[16]. X. Gao, O. Edfors, F. Rusek, F. Tufvesson, Linear pre-coding performance in measured very large MIMO channels, in *Proceedings of the IEEE Vehicular Technology Conference (VTC Fall)*, 2011, pp. 1-5.

[17]. R. S. Dhar, S. G. Razavipour, E. Dupont, Z. Wasilewski, et al., Scanning voltage microscopy study of lasing and non-lasing terahertz quantum cascade lasers, in *Proceedings of the Conference on Lasers and Electro-Optics (CLEO)*, 2015, STu1G.4.

[18]. C. Masouros, M. Sellathurai, T. Ratnarajah, Large-scale MIMO transmitters in fixed physical spaces: The effect of transmit correlation and mutual coupling, *IEEE Transactions on Communications*, Vol. 61, Issue 7, 2013, pp. 2794-2804.

[19]. R. S. Dhar, D. Ban, Nanoscopic voltage distribution of operating cascade laser devices in cryogenic temperature, *Journal of Microscopy*, Vol. 262, Issue 3, 2016, pp. 226-231.

[20]. C. Masouros, J. Chen, K. Tong, M. Sellathurai, et al., Towards massive MIMO transmitters: On the effects of deploying increasing antennas in fixed physical space, in *Proceedings of the Future Network & Mobile Summit*, 2013, pp. 1-10.

[21]. G. S. Sahoo, A. Ghosh, Antenna array design for higher spectral efficiency for hybrid beamforming 5G MIMO wireless communication system, in *Proceedings of the IEEE Wireless Antenna and Microwave Symposium (WAMS)*, 2022, pp. 1-5.

[22]. R. Singh, P. Chawla, Performance analysis of OMP hybrid beamforming algorithm for OFDM millimeter-wave MIMO systems, in *Proceedings of the International Conference on Computing, Communication and Power Technology (IC3P)*, 2022, pp. 71-74.

[23]. R. S. Dhar, C. Xu, D. Ban, L. Li, et al., Direct observation of non-uniform electric field in the active regions of an interband cascade laser, in *Proceedings of the Conference on Lasers and Electro-Optics (CLEO)*, 2014, STh3G.3.

[24]. D. Ying, F. W. Vook, T. A. Thomas, D. J. Love, Hybrid structure in massive MIMO: Achieving large sum rate with fewer RF chains, in *Proceedings of the IEEE International Conference on Communications (ICC)*, 2015, pp. 2344-2349.

[25]. F. Sohrabi, W. Yu, Hybrid analog and digital beamforming for mmWave OFDM large-scale antenna arrays, *IEEE Journal on Selected Areas in*

*Communications*, Vol. 35, Issue 7, 2017, pp. 1432-1443.

[26]. L. Dai, X. Gao, J. Quan, S. Han, et al., Near-optimal hybrid analog and digital precoding for downlink mmWave massive MIMO systems, in *Proceedings of the IEEE International Conference on Communications (ICC)*, 2015, pp. 1334-1339.

[27]. Z. C. Phyo, A. Taparugssanagorn, Hybrid analog-digital downlink beamforming for massive MIMO system with uniform and non-uniform linear arrays, in *Proceedings of the 13th International Conference on Electrical Engineering/Electronics, Computer, Telecommunications and Information Technology (ECTI-CON)*, 2016, pp. 1-6.

[28]. L. Leyva, D. Castanheira, A. Silva, A. Gameiro, Hybrid beamforming design for communication-centric ISAC, *IEEE Sensors Journal*, Vol. 24, Issue 15, 2024, pp. 24567-24579.

[29]. D. H. N. Nguyen, L. B. Le, T. Le-Ngoc, R. W. Heath, Hybrid MMSE precoding and combining designs for mmWave multiuser systems, *IEEE Access*, Vol. 5, 2017, pp. 19167-19181.

[30]. O. El Ayach, S. Rajagopal, S. Abu-Surra, Z. Pi, et al., Spatially sparse precoding in millimeter-wave MIMO systems, *IEEE Transactions on Wireless Communications*, Vol. 13, Issue 3, 2014, pp. 1499-1513.

[31]. Y. Chen, D. Chen, T. Jiang, L. Hanzo, Millimeter-wave massive MIMO systems relying on generalized sub-array-connected hybrid precoding, *IEEE Transactions on Vehicular Technology*, Vol. 68, Issue 9, 2019, pp. 8940-8950.

[32]. P.-A. Absil, R. Mahony, R. Sepulchre, Optimization Algorithms on Matrix Manifolds, *Princeton University Press*, Princeton, 2008.

[33]. D. H. N. Nguyen, L. B. Le, T. Le-Ngoc, Hybrid MMSE precoding for mmWave multiuser MIMO systems, in *Proceedings of the IEEE International Conference on Communications (ICC)*, 2016, pp. 1-6.

[34]. X. Yu, J.-C. Shen, J. Zhang, K. B. Letaief, Alternating minimization algorithms for hybrid precoding in millimeter-wave MIMO systems, *IEEE Journal of Selected Topics in Signal Processing*, Vol. 10, Issue 3, 2016, pp. 485-500.

[35]. J. Cong, T. Lin, Y. Zhu, Hybrid MMSE beamforming for multiuser millimeter-wave communication systems, *IEEE Communications Letters*, Vol. 22, Issue 11, 2018, pp. 2390-2393.

[36]. J. Lee, Y. H. Lee, AF relaying for millimeter-wave communication systems with hybrid RF/baseband MIMO processing, in *Proceedings of the IEEE International Conference on Communications (ICC)*, 2014, pp. 5838-5842.

[37]. V. Stankovic, M. Haardt, Generalized design of multi-user MIMO precoding matrices, *IEEE Transactions on Wireless Communications*, Vol. 7, Issue 3, 2008, pp. 953-961.

[38]. P. R. Gautam, L. Zhang, Hybrid precoding for millimeter-wave MIMO: Trace optimization approach, *IEEE Access*, Vol. 10, 2022, pp. 66874-66885.

[39]. Y. Chen, D. Chen, T. Jiang, L. Hanzo, Channel-covariance and angle-of-departure aided hybrid precoding for wideband multiuser millimeter-wave MIMO systems, *IEEE Transactions on Communications*, Vol. 67, Issue 12, 2019, pp. 8315-8328.

[40]. Y. Chen, Y. Xiong, D. Chen, T. Jiang, et al., Hybrid precoding for wideband millimeter-wave MIMO systems in the face of beam squint, *IEEE Transactions on Wireless Communications*, Vol. 20, Issue 3, 2021, pp. 1847-1860.

[41]. Y. Chen, D. Chen, Y. Tian, T. Jiang, Spatial lobes division-based low-complexity hybrid precoding and diversity combining for mmWave IoT systems, *IEEE Internet of Things Journal*, Vol. 6, Issue 2, 2019, pp. 3228-3239.

[42]. T. Kebede, Y. Wondie, J. Steinbrunn, H. B. Kassa, et al., Precoding and beamforming techniques in mmWave-massive MIMO: Performance assessment, *IEEE Access*, Vol. 10, 2022, pp. 16365-16387.

[43]. W. Park, J. Choi, Hybrid precoding and combining strategy for MMSE-based rate balancing in mmWave multiuser MIMO systems, *IEEE Access*, Vol. 10, 2022, pp. 88043-88057.

[44]. G. M. Zilli, W.-P. Zhu, Constrained-SVD based hybrid beamforming design for millimeter-wave communications, in *Proceedings of the 92nd IEEE Vehicular Technology Conference (VTC Fall)*, 2020, pp. 1-5.

[45]. K. Ying, Z. Gao, S. Lyu, Y. Wu, et al., GMD-based hybrid beamforming for large reconfigurable intelligent surface assisted millimeter-wave massive MIMO, *IEEE Access*, Vol. 8, 2020, pp. 19530-19539.

[46]. A. Alkhateeb, R. W. Heath, Gram-Schmidt based greedy hybrid precoding for frequency-selective millimeter-wave MIMO systems, in *Proceedings of the IEEE International Conference on Acoustics, Speech and Signal Processing (ICASSP)*, 2016, pp. 3396-3400.

Published by International Frequency Sensor Association (IFSA) Publishing, S. L., 2026 (http://www.sensorsportal.com).